7. Xia, J., Miller, R. D. and Park, C. B., Estimation of near-surface shear-wave velocity by inversion of Rayleigh waves. *Geophysics*, 1999, **64**, 691–700.
8. Richart, F. E., Hall, J. R. and Woods, R. D., *Vibrations of Soils and Foundations*, Prentice-Hall, 1970.
9. Xia, J., Miller, R. D. and Park, C. B., Advantages of calculating shear wave velocity from surface waves with higher modes, SEG, Expanded Abstracts, 2000.
10. Park, C. B., Miller, R. D. and Xia, J., Offset and resolution of dispersion curve in multichannel analysis of surface waves (MASW). In Proceedings of the SAGEEP, Denver, Colorado, RBA-6, 2001.
11. Ryden, N., Park, C., Miller, R., Xia, J. and Ivanov, J., High frequency MASW for non-destructive testing of pavements. In Proceedings of the Symposium on the Application of Geophysics to Engineering and Environmental Problems, Denver, Colorado, 4–7 March 2001.
12. Ivanov, J., Park, C. B., Miller, R. D. and Xia, J., Mapping Poission's ratio of unconsolidated materials from a joint analysis of surface-waves and refraction events. In Proceedings of the Symposium on the Application of Geophysics of Engineering and Environment Problems, Arlington, VA, 20–24 February 2000.
13. Park, C. B., Miller, R. D., Xia, J. and Ivanov, J., Multichannel analysis of underwater surface wave near B. C. Vancouver, Canada. In Proceedings of the 70th Annual International Meeting, SEG, Expanded Abstracts, 2000, pp. 1303–1306.
14. Miller, R. D., Xia, J., Park, C. B. and Ivanov, J., Multichannel analysis of surface waves to map bedrock. *Leading Edge*, 1999, **18**, 1392–1396.
15. Miller, R., Xia, J., Park, C. B., Davis, J., Shefchik, W. and Moore, L., Seismic techniques to delineate dissolution features in the upper 1000 ft at a power plant. In 69th Annual International Meeting, SEG, Expanded Abstracts, 1999, pp. 492–495.
16. FEMA, Multi hazard identification and assessment, Federal Emergency Management Agency, Washington DC, USA, 1997.
17. International Building Code, International Code Council, Falls Church, VA, 2000, 5th edn.
18. Konno, K. and Ohmachi, T., Ground motion characteristics estimated from spectral ratio between horizontal and vertical components of microtremor. *Bull. Seismol. Soc. Am.*, 1998, **88**(1), 228–241.
19. Bonilla, L. F., Steidl, J. H., Lindley, G. T., Tumarkin, A. G. and Archuleta, R. J., Site amplification in the San Fernando Valley, California; variability of site effect estimation using the *S*-wave, Coda, and *H*/*V* methods. *Bull. Seismol. Soc. Am.*, 1997, **87**(3), 710–730.
20. Field, E. and Jacob, E. H., A comparison and test of various site response techniques, including three that are non-reference-site dependent. *Bull. Seismol. Soc. Am*., 1995, **85**, 1127–1143.
21. Castr, R. R., Mucciarelli, M., Pacor, F. and Petrungaro, C., *S*-wave site response using horizontal-to-vertical spectral ratios. *Bull. Seismol. Soc. Am*., 1997, **87**(1), 256–260.
22. Bonilla, L. F., Steidl, J. H., Lindley, G. T., Tumarkin, A. G. and Archuleta, R. J., Borehole response studies at the Garner valley, southern California. *Bull. Seismol. Soc. Am.*, 2002, **92**(8), 3165–3379.
23. Lermo, J. and Chavez-Garcia, F. J., Are microtremors useful in site response evaluation? *Bull. Seismol. Soc. Am*., 1994, **84**, 1350–1364.

ACKNOWLEDGEMENT. We thank Dr T. Sheshunarayan, NGRI, Hyderabad for guidance in the acquisition of data, processing and interpretation.

Received 9 December 2009; revised accepted 9 December 2010

Characterization of reflectance spectra of lunar analog rocks: gabbro and norite

S. Arivazhagan and S. Anbazhagan*

Department of Geology, Periyar University, Salem 636 011, India

Gabbro and noritic rocks are of particular interest to lunar scientists because they stratigraphically represent the deeper zones of the lunar crust. This communication reports reflectance spectra under 350–2500 nm for lunar analog rocks like gabbro and norite and a comparison with mineralogy and chemical composition. The gabbro and norite distinctly vary in terms of albedos of reflectance spectra. However, these rocks have common absorption bands in the visible–near infrared and SWIR spectral range. Norite has pyroxene absorption at 1072 nm, whereas this absorption is absent in gabbro. Similarly, the broader absorption band at 1200 nm in gabbro is probably due to overlapping absorption by crystalline plagioclase feldspar and the presence of pyroxene. Overall, minor variation in absorption bands, percentage of albedos and band depth are the diagnostic features useful for remote mapping of similar rock types on the lunar surface.

Keywords: Gabbro, norite, reflectance spectra, lunar analog.

A WIDE variety of rock types exist throughout the near-side crust of the moon. Major rock types identified from the reflectance spectra include noritic, anorthositic, gabbroic and troctolitic composition[1]. The lunar crust exhibits noritic composition with different amounts of pyroxene and/or brecciation alteration. Materials representing stratigraphically deeper zones (5–15 km) of the lunar crust are dominated by gabbros, anorthosites and troctolites, with less than a quarter of the areas exhibiting noritic composition[1]. The noritic character of lunar breccias and glasses was recognized during the study of Apollo 11 and 12 samples[2,3]. It is assumed that the lunar crust is stratified into distinct upper anorthositic and lower noritic layers[4]. The dominant rock type noticed across the interior of the South Pole-Aitken basin is of noritic composition[5], representing lower crust mafic suite. The lunar highland region comprises of >90% plagioclase (anorthite). In some cases between 10% and 22.5% mafic composition (orthopyroxene, clinopyroxene or olivine) with the remainder plagioclase (noritic anorthosite, gabbroic anorthosite and troctolitic anorthosite); or between 22.5% and 40% mafic with the remainder plagioclase (anorthositic norite, anorthositic gabbro and anorthositic troctolite), and more than 40% mafic (norite,

*For correspondence. (e-mail: anbu02@gmail.com)

gabbro and troctolite)[1]. Gabbroic rocks are concentrated in the western hemisphere of the lunar near side[1]. Planetary remote sensing, particularly for lunar exploration, is an emerging field useful for the geological and mineral mapping of the lunar surface. Remote sensing experiments analysing the sunlight reflected by planetary surfaces can be used to derive the mineralogical composition[6] and physical properties[7] of the natural surfaces. Several countries are planning to map the lunar surface through remote orbiters and explore the subsurface through rovers. The imaging spectrometry in the visible and NIR on-board spacecraft has become an essential technique to study the surface and atmosphere of planetary objects, prior and in addition to *in situ* analyses[8]. Remote spectroscopy is one of the most powerful techniques to observe and study the chemistry and mineralogy of interest on the surface of extraterrestrial planets. On the basis of the characteristic absorption bands for known minerals, distinct rock types have been identified. A simple technique to qualitatively evaluate remote spectra is to compare them with laboratory reference spectra[9,10]. In this context, the terrestrial gabbro and norite are considered as lunar analog rocks and the reflectance spectra were studied and characterized for remotely mapping the rock types on the lunar crust.

Gabbro and norite samples of size 5″ × 5″ were used for measuring the reflectance spectra. In order to avoid the hydration process in terrestrial samples, fresh samples were taken for spectral, mineralogy and chemical studies. Gabbro is a dense, greenish, dark-coloured plutonic rock with clino pyroxene, Ca-rich plagioclase feldspar, amphibole and olivine with accessories of opaque minerals. Gabbro is generally coarse-grained with ophitic texture. Norite is a mafic intrusive igneous rock composed of calcium plagioclase, ortho pyroxene with olivine. Thin sections were prepared to study the mineralogy (Figures 1 and 2). The major minerals in the terrestrial gabbro are pyroxene (diopside, hypersthene), plagioclase feldspar, amphibole, quartz and opaques like hematite and ilmenite. The minerals observed in the norite thin section are pyroxene (hypersthene, diopside), hornblende and accessories of hematite and ilmenite. The lunar gabbro and norite have high amount of pyroxenes (both clino and ortho) when compared to the terrestrial rocks. Similarly, the plagioclase content is equally significant in the lunar gabbro and norite samples.

Apart from microscopic studies, a portion of the samples was used for chemical analysis. The chemical compositions of the terrestrial gabbro and norite were compared with the lunar gabbro and norite chemical compositions (Table 1). The results of chemical analyses of lunar gabbro, lunar gabbro–norite, lunar norite, shocked anorthositic norite and lunar olivine norite are presented in Table 2 (refs 11–13). The percentage of oxide in lunar gabbros mostly matches with the analog gabbros like SiO_2, TiO_2, Al_2O_3 and CaO, except for a major variation in the content of FeO and Fe_2O_3. Overall, the lunar gabbro has high mafic content. The analog norite also shows similarity with lunar samples in the case of major oxides, such as SiO_2, Al_2O_3, MgO and CaO. The common feature encourages characterizing the spectra of terrestrial rock samples as analogs to the lunar geology. Similar analog studies for the lunar mare basalt[14] and highland region[15] have shown appreciable results.

Measurements of the reflected light within the visible, NIR and SWIR wavelength ranges represent a powerful approach to the analysis of igneous rocks. The technological improvement of spatial and spectral resolution of sensors on aerial and space platforms and developments in planetary research have encouraged scientists to take up laboratory and field spectroscopic studies for modelling the terrestrial analogs of planetary surfaces[16]. Several studies have been made in the past 30 years on the electronic nature of the absorption of light occurring in the

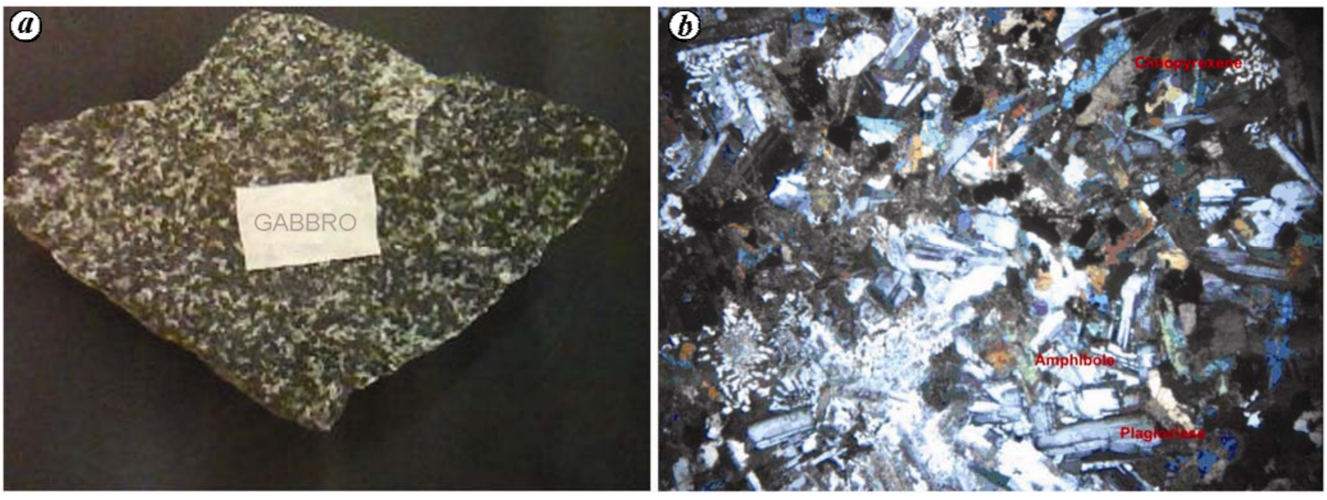

Figure 1. Gabbro hand specimen (***a***) and the photomicrograph (***b***) showing the ophitic texture with plagioclase and clinopyroxene being the major minerals and biotite the minor mineral.

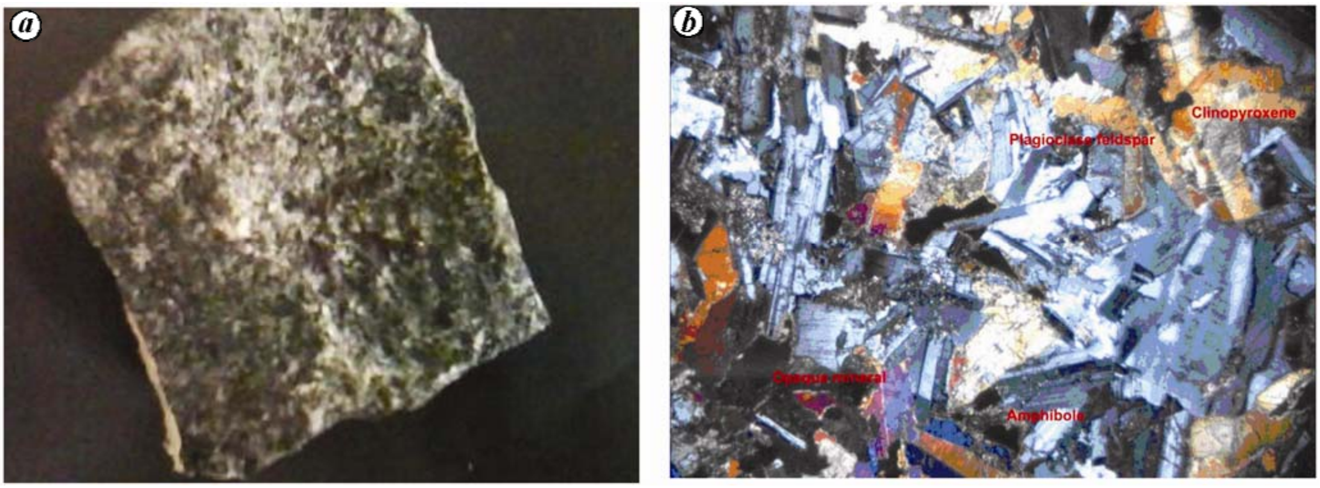

Figure 2. Norite hand specimen (***a***) and photomicrograph (***b***) showing the ophitic texture with plagioclase and hypersthene pyroxene as the major minerals.

Table 1. Chemical analysis of oxides of analog rocks, lunar gabbro and norite

Percentage of oxides	Gabbro[a]	Lunar gabbro[b]	Lunar gabbro–norite[b]	Norite[a]	Lunar norite[b]	Shocked anorthositic norite[c]	Lunar olivine norite[c]
SiO_2	52.4	48.39	50.7	51.32	51.1	45.31	46.07
TiO_2	2.37	0.9	0.4	0.89	0.33	0.36	0.26
Al_2O_3	13.72	8.85	13.2	15.32	15	20.44	26.18
FeO	–	20.68	9.91	–	9.9	12.6	6.68
Fe_2O_3	16.03	–	–	12.72	–	–	–
MgO	3.77	7.79	12.8	6.19	12.5	6.88	4.43
MnO	0.18	0.33	–	0.17	–	0.19	0.11
CaO	7.69	12.13	11.6	10.48	9.1	14.41	15.86
Na_2O	2.98	0.21	0.91	2.23	0.4	0.15	0.26
K_2O	1.48	0.01	0.017	0.46	0.173	0.01	0.06
P_2O_5	0.64	0.02	–	0.11	–	–	–
Total	101	99.31	99.537	99.890	98.50	100.35	99.91

[a]Terrestrial gabbro and norite, India. [b]BVSP[11]. [b]Ref. 12. [c]Ref. 13.

VNIR spectra of transition metal-bearing minerals[6,17–28]. Several approaches to spectral analysis have been developed and successfully used to infer the presence of minerals with distinctive spectral signatures. Empirical approaches have been used to find out the relationships between spectroscopic and compositional parameters, both chemical and mineralogical components using laboratory measurements of terrestrial analogs. Band minima of rock spectra are strongly influenced by the concurrent effects due to modal abundance of the spectroscopically active minerals and chemistry.

In the present study spectral measurements were directly acquired on solid rock-slab surfaces in the VNIR and SWIR range. Common parametric measurements of spectral reflectance include the albedo, the total amount of light reflected. Reflectance spectra were obtained under two different environments, viz. controlled field condition and in the laboratory. The measurements were carried out on the terrace of a building referred to as controlled field condition and in such an environment certain parameters were kept under control to avoid errors. The board coated with $BaSO_4$ was used for instrument calibration[29]. Spectral measurements were taken using optical fibre cable at a height of 30 cm with 1° field-of-view under clear atmospheric condition. The height and angle of the optical fibre were kept constant. Moreover, the samples were placed over a black card-board paper to avoid irradiance from the surroundings. However, atmospheric interruption is inevitable in the controlled field condition near 1450 and 1800 nm. The reflectance spectra measured under controlled field condition are useful to be compared with the laboratory spectra.

The directional–hemispherical reflectance spectra from rock slab surfaces were collected using halogen lamp as the source light in the laboratory. Under laboratory condition, a clear spectrum was obtained for both the rock

Table 2. Mineralogy of analog rocks, and lunar gabbro and norite

Percentage of minerals	Gabbro	Lunar gabbro	Lunar gabbro–norite	Norite	Lunar norite	Lunar olivine norite	Shocked anorthositic norite
Quartz	11.43	0.633	–	9.232	3.144	0.102	–
Orthoclase	9.045	0.062	0.100	2.789	1.034	0.358	0.060
Plagioclase	48.047	26.501	39.993	51.778	42.727	73.105	57.273
Diopside	5.571	31.193	20.504	15.113	5.283	6.940	13.336
Olivine	–	–	2.889	–	–	–	10.203
Hypersthene	7.984	40.241	35.957	9.984	47.347	19.129	18.618
Hematite	11.557	–	–	9.097	–	–	–
Ilmenite	0.292	1.326	0.557	0.274	0.465	0.366	0.509
Sphene	4.687	–	–	1.498	–	–	–
Apatite	1.384	1.384	–	0.236	–	–	–
Total	99.997	101.34	100	100.001	100	100	99.999

Table 3. Reflectance percentage (albedo) of lunar analog rocks: gabbro, norite, anorthosite and basalt

Spectral region	Gabbro (%)	Norite (%)	Basalt[a] (%)	Anorthosite[b] (%)
VIS	10–11	8–9	4–7	20–26
NIR	11–14	9–10	7–8	26–29
SWIR	14–15	9–10	6–7	25–31

[a]Ref. 14. [b]Ref. 15.

samples. We can clearly distinguish the two rock types with a number of intermediate spectral morphologies, according to the overall spectral shape and appearance of diagnostic absorption features. The laboratory spectra of gabbro and norite are shown in Figures 3 *a* and 4 *a* respectively.

The empirical evaluation of solid rock surface spectra needs further insights for improvement in planetary researches. In addition, genetic sequences of rocks should be studied in detail to help in the geological interpretation of planetary evolution. Therefore, more laboratory and analytical studies are required to understand the influence of composition and petrographic textures on the spectral analysis. Detailed examination of solid rock spectra is still in a developmental stage[30–33].

Rocks are complex natural systems with extremely variable texture, chemistry, crystal structure and combinations of these parameters. Keeping this in mind, we have collected detailed information on the chemistry and mineralogy of the rocks, using methods other than spectroscopy.

A number of minor absorption bands that occur between 400 and 600 nm in a rock are generally attributed to spin-forbidden crystal field transitions in Fe^{2+}/Mn^{2+} crystallographic sites[6,17,27,34–36]. Pyroxene and plagioclase are the common constituents of extraterrestrial materials, widespread on terrestrial planetary surfaces as the main rock-forming minerals of both bedrocks and regolith. Since pyroxene, plagioclase and ilmenite are anhydrous minerals, the sharp and narrow vibrational absorptions occurring in the NIR wavelength range are generally attributed to minerals derived from hydration and hydroxylation of the primary phases. The bands are ubiquitous within the rock spectral series and occur at/near ~1400, ~1900, ~2200, ~2250 and ~2330 nm. Absorption features due to metal-OH vibrational transitions in minerals are generally closely spaced within the wavelength interval between 2000 and 2500 nm. Absorptions due to molecular vibrations within the crystal lattice occur near 1400 nm (2*n*OH hydroxyl overtone), 1900 nm ($n2 + n3$ combination mode of molecular water), 2200 and 2300 nm (Al^{3+}–OH and Mg^{2+}–OH stretches and bends)[27]. Several techniques such as parabolic correction, continuum removal, interpretation of albedos and absorption features are involved in analysis of spectral data. The spectrally processed and continuum-removed reflectance spectra of gabbro and norite are shown in Figures 3 *b* and 4 *b*.

The percentage and range of reflectance (albedos) in different parts of the spectrum vary for different rock types. In the present analog samples, the percentage of reflectance for gabbro varied from 13 in the visible spectrum to 15 in the SWIR spectrum. However, norite has slightly low albedos than gabbro, and it ranged from 8% to 9% in the visible spectrum, and 9% to 10% in the NIR and SWIR region (Table 3; Figures 3 *a* and 4 *a*). Similarly, the reflectance percentage differs for other lunar analog rocks such as anorthosites and basalts[14,15].

Gabbro has absorption spectra at 378, 1200, 1407, 1790, 1912, 2205, 2262 and 2340 nm (Figure 3 *a*). The continuum-removed reflectance spectra of gabbro are plotted in Figure 3 *b*. Though the depth of absorption features is different in both plots, the absorption band centres are more or less located in the same wavelength. Reflectance spectra of gabbro collected from the spectral library at Johns Hopkins University, USA, are shown in Figure 3 *c*. It should be noted that the library spectra are plotted in the wider wavelength range of 350 nm–14 μm. However, under 350–2500 nm, the absorption bands of the terrestrial analog gabbro match with those of the spectral library gabbro under the same range (Figure 3 *c*). Compared to gabbro, norite has low albedos with featureless spectra. It has weak absorptions at 378, 693, 1072, 1411, 1949, 2200 and 2337 nm (Figure 4 *a*). The library spectra for norite collected from JHU also shows similar absorption features (Figure 4 *c*).

The weak absorption near 378 nm is due to the contribution of small amounts of Fe^{3+} (refs 22 and 37). The visible wavelength regions of calcium pyroxene reflectance spectra exhibit a number of absorption bands which are attributable to Fe^{2+} spin forbidden crystal field transitions. Fe^{2+} and Fe^{3+} intervalance charge transfer absorption bands near 770 nm are common in terrestrial pyroxene which contains both ferrous and ferric iron[27]. High-calcium pyroxene (HCP) spectra can be broadly assigned to one of the two types on the basis of their absorption bands[27]. If the sample contains >50% of wollastonite (within pyroxene), it is considered as HCP, and if it contains less than 50%, it is considered as low calcic pyroxene.

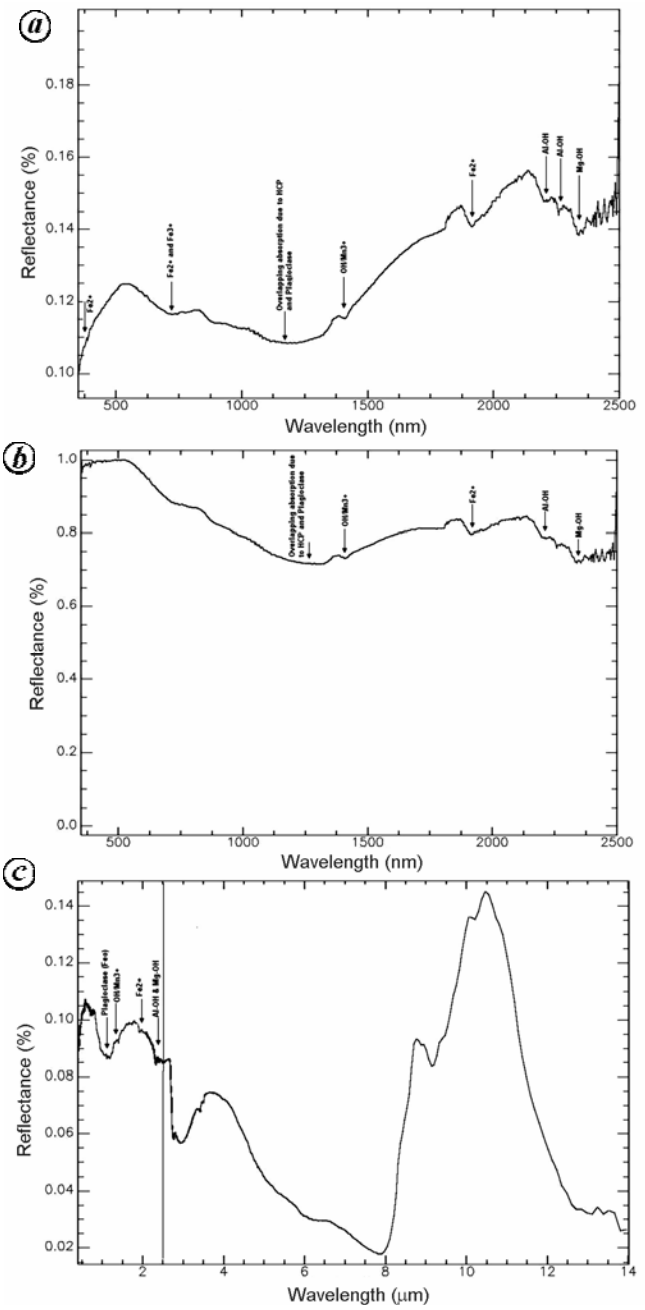

Figure 3. Reflectance spectra of gabbro in laboratory condition (***a***), continuum-removed reflectance spectra (***b***) and gabbro spectra from the Johns Hopkins University spectral library (***c***).

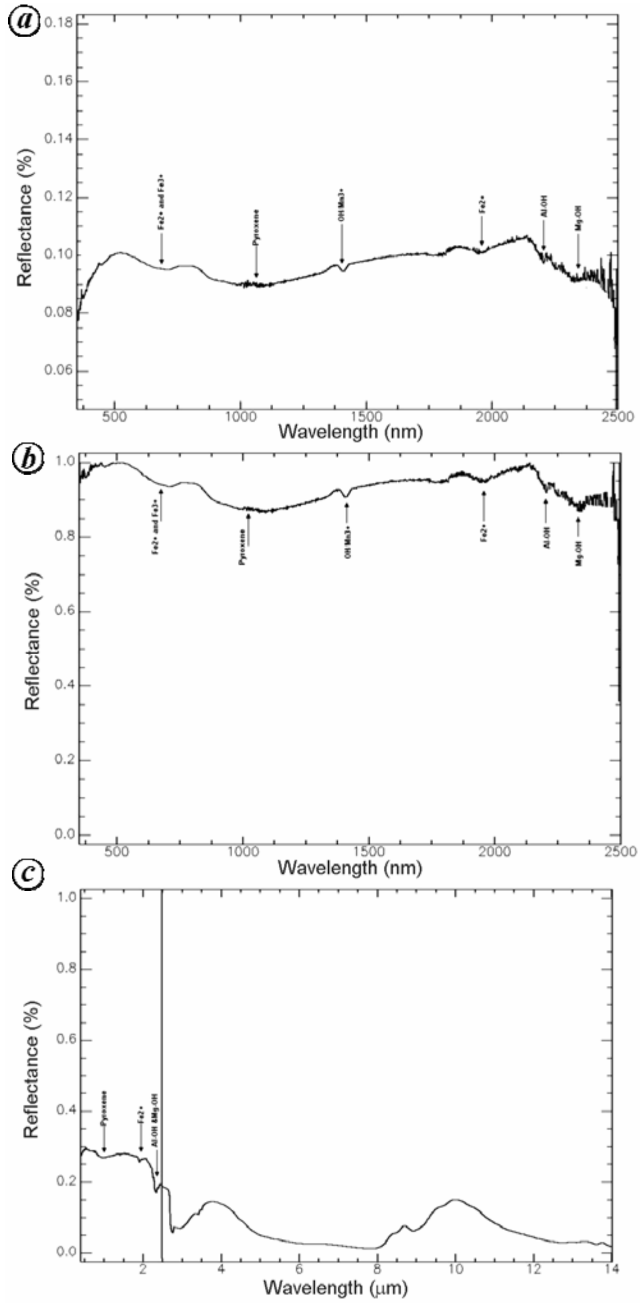

Figure 4. Reflectance spectra of norite in laboratory condition (***a***), continuum-removed reflectance spectra (***b***) and norite spectra from Johns Hopkins University spectral library (***c***).

Table 4. Absorption band depths for lunar analog rocks: gabbro and norite in the 350–2500 nm wavelength region

	Band depth		
Wavelength (nm)	Analog gabbro	Analog norite	Causes
700	–	0.06435	Fe^{2+} and Fe^{3+} intervalance charge transfer absorption
1040	–	0.07581	Pyroxene absorption
1200	0.282	–	Plagioclase (FeO) absorption
1400	0.0118	0.02052	OH/Mn^{3+} crystal transition
1915	0.0482	0.02938	Ferrous iron/ H_2O
2200	0.0773	0.92955	Al–OH absorption
2260	0.0326	–	Al–OH absorption
2330	0.0523	0.05035	Mg–OH vibration spectra

In the present analog study, though both gabbro and norite have pyroxene, the percentage of ca-pyroxene is high in the case of norite (>50%). With increase in calcium and iron contents in pyroxene, the absorption band centres shift in a regular manner to longer wavelength (i.e. >0.98 μm)[18]. The broad absorption at 1072 nm in norite indicates the presence of HCP. The broad absorption at 1200 nm in gabbro is significant, which indicates low-calcium pyroxene and the dominance of Fe^{2+} crystalline plagioclase feldspar which has inflection near 1.25 μm. Pyroxene is identified by the existence of paired absorption bands near 1 and 2 μm (refs 18 and 38). In the present analog rock samples, the absorptions at 1912 and 1949 nm for gabbro and norite indicate the pyroxene absorptions. The absorptions near 2.2 and 2.35 μm are due to the hydroxyl and Al–OH, Mg–OH elements in both analog rock samples. Gabbroic spectra exhibit characteristic pyroxene absorption bands only at 1912 nm. Most gabbroic rocks exhibit a notable inflection near 1.25 μm, indicating the presence of a significant crystalline Fe-bearing plagioclase component. This composition of type gabbroic is general in nature, although pyroxene abundance will be beyond a minimum of 10–12%. In the present context, the broad absorption at 1200 nm is due to multiple overlapping absorption components due to the presence of high percentage of Fe-bearing plagioclase and calcium clino pyroxene in gabbro.

In addition to albedo, absorption band centres, the absorption depths are also considered as diagnostic features for different minerals and rocks. The absorption depth is calculated from continuum-removed spectra using the formula[39]

$$D = 1 - Rb/Rc, \quad (1)$$

where D is the band depth, Rb the reflectance at the bottom and Rc the reflectance at the continuum. The absorption band depths calculated for different absorption band centres for analog gabbro and norites are presented in Table 4. The absorption depths vary for gabbro, norite and other analog rocks such as basalts and anorthosites.

Though the terrestrial analogs have similar chemical composition and absorption spectra with lunar gabbro and norite to some extent, it is necessary to understand the space weathering due to solar flux. The importance of space weathering for implications of geological studies on planetary surface has been discussed earlier[40,41]. Space weathering due to solar flux induces development of lunar regolith and soil maturity. Space weathering alters the spectra, like decrease of albedo, reduction in the spectral contrast and increase of continuum slope in the longer wavelength[41–47]. In order to understand the effect of space weathering on the spectra, experimental simulation study of lunar surface process could be useful[48,49]. Similarly, the surface effect can be removed by development of algorithms from the input of lunar-returned soils and remote sensing data[40].

The reflectance characteristics of the analog rocks and minerals are important for remotely mapping of planetary surfaces. Advances in imaging spectrometer technology allow better spectral and spatial resolution, increasing the requirements for understanding the spectral properties of proper analogs of planetary surfaces, which are likely to include solid rocks. Further studies are required to address the spectral effects due to more complicated rock texture. The analog gabbro and norite spectra were compared with the JHU spectral library data. The analog gabbro and norite have similar spectra and common absorption bands as the library spectra.

Norite has low albedos (8–10%) than gabbro and anorthosite, and also relatively featureless spectrum when compared to gabbro. Similarly, the absorption depths also differ for norite. These diagnostic features are useful in discriminating the norite (lower crust), gabbro (deeper zones of lunar crust), anorthosite (upper crust) and basalt.

Table 1 shows the lunar gabbro and norite samples with minor variation in chemical composition. In some samples, only minor variations were observed in the chemical composition of oxides of lunar gabbro and norite. The terrestrial analog samples also have similar chemical composition. It is inferred that the spectral characteristics of analog gabbro and norite are probably influenced by the concentration of mafic minerals such as iron, magnesium and the percentage of calcium minerals. It is necessary to have more analog samples along with chemical data for better understanding of spectral behaviour of analog rocks. The comparison of analog spectra with lunar empirical data such as Clementine and Chandrayaan 1 spectra, will give further insight to characterize the spectra of analog rocks. The knowledge of spectral variation due to space weathering process may improve remote sensing studies of lunar surface.

1. Pieters, C. M., Composition of the lunar highland crust from near-infrared spectroscopy. *Rev. Geophys.*, 1986, **24**, 557–578.
2. Prinz, M., Bunch, T. E. and Keil, K., Composition and origin of lithic fragments and glasses in Apollo II samples. *Contrib. Mineral. Petrol.*, 1971, **32**, 211–230.
3. Wood, J. A., Fragments of tetra rock in the Apollo 12 soil samples and a structural model of the moon. *Icarus*, 1972, **16**, 462–501.
4. Wieczorek, M. A. and Zuber, M. T., The composition and origin of the lunar crust: constraints from central peaks and crustal thickness modeling. *Geophys. Res. Lett.*, 2001, **28**, 4023–4026.
5. Pieters, C. M., Tompkins, S., Head, J. W. and Hess, P. C., Mineralogy of the mafic anomaly in the South Pole-Aitken Basin: Implications for excavation of the lunar mantle. *Geophys. Res. Lett.*, 1997, **24**, 15, 1903–1906.
6. Burns, R. G., *Mineralogical Applications of Crystal Field Theory*, Cambridge University Press, New York, 1993, 2nd edn, p. 551.
7. Pieters, C. M. and Englert, P. A. J. (eds), *Remote Geochemical Analysis: Elemental and Mineralogical Composition*, Cambridge University Press, New York, 1997, pp. 312–317.
8. Bonello, G., Bibring, J. P., Morris, R. V. and Mustard, J. F., OMEGA observation of Mars analogue rocks. *Lunar Planet. Sci.*, 2003, **XXXIV**, 1664.pdf.
9. Gaffey, M. J., Lebofsky, L., Nelson, M. and Jones, T., Asteroid surface composition from earth-based reflectance spectroscopy. In *Remote Geochemical Analysis: Elemental and Mineralogical Composition* (eds Pieters, C. M. and Englert, P. A. J.), Cambridge University Press, New York, 1993, pp. 437–453.
10. Pieters, C. M., Mustard, J. F. and Sunshine, J. M., Quantitative mineral analyses of planetary surfaces using reflectance spectroscopy. In *Mineral Spectroscopy: A Tribute to Roger G. Burns* (eds Dyars, M. D., McCammon, C. and Schaefer, M. W.), Special Publication No. 5, Geochemical Society, Houston, Texas, 1996, pp. 307–325.
11. BVSP, *Basaltic Volcanism Study Project: Basaltic Volcanism on the Terrestrial Planets*, Pergamon Press, 1981, p. 1286.
12. Heiken, G. H., Vaniman, D. T. and French, B. M. (eds), *Lunar Sourcebook*, Cambridge University Press, Cambridge, 1991, p. 736.
13. Donnel, S. P., Jolliff, B. L., Zeigler, R. A. and Korotev, R. L., Identifying the Mafic components in Lunar regolith breccia NW 3136. *Lunar Planet. Sci.*, 2008, **XXXIX**, 2507.pdf.
14. Anbazhagan, S. and Arivazhagan, S., Reflectance spectra of analog basalts; implications for remote sensing of lunar geology. *Planet. Space Sci.*, 2009, **57**, 1346–1358.
15. Anbazhagan, S. and Arivazhagan, S., Reflectance spectra of analog anorthosites; implications for lunar highland mapping. *Planet. Space Sci.*, 2009, **58**, 752–760.
16. Pompilio, L., Sgavetti, M. and Pedrazzi, G., Visible and near-infrared reflectance spectroscopy of pyroxene-bearing rocks: New constraints for understanding planetary surface compositions. *J. Geophys. Res.*, 2007, **112**, E01004.
17. Burns, R. G., *Mineralogical Applications of Crystal Field Theory*, Cambridge University Press, New York, 1970, p. 224.
18. Adams, J. B., Visible and near-infrared diffuse reflectance spectra of pyroxenes as applied to remote sensing of solid objects in the solar system. *J. Geophys. Res.*, 1974, **79**, 4829–4836.
19. Nitsan, U. and Shankland, T. J., Optical properties and electronic structure of mantle silicates. *Geophys. J. R. Astron. Soc*., 1976, **45**, 59–87.
20. Cloutis, E. A., Gaffey, M. J., Jackowski, T. L. and Reed, K. L., Calibrations of phase abundance, composition and particle size distribution of olivine–orthopyroxene mixtures from reflectance spectra. *J. Geophys. Res.*, 1986, **91**, 11,641–11,653.
21. King, T. V. V. and Ridley, W. I., Relation of the spectroscopic reflectance of olivine to mineral chemistry and some remote sensing implications. *J. Geophys. Res*., 1987, **92**, 11457–11469.
22. Wagner, J. K., Hapke, B. W. and Wells, E. N., Atlas of reflectance spectra of terrestrial, lunar and meteoritic powders and frosts from 92 to 1800 nm. *Icarus*, 1987, **69**, 14–28.
23. Cloutis, E. A. and Gaffey, M. J., Pyroxene spectroscopy revisited: spectral–compositional correlations and relationships to geo thermometry. *J. Geophys. Res*., 1991, **96**, 22809–22826.
24. Straub, D. W., Burns, R. G. and Pratt, S. F., Spectral signature of oxidized pyroxenes: Implications to remote sensing of terrestrial planets. *J. Geophys. Res.*, 1991, **96**, 18819–18830.
25. Sunshine, J. M. and Pieters, C. M., Estimating modal abundances from the spectra of natural and laboratory pyroxene mixtures using the modified Gaussian model. *J. Geophys. Res.*, 1993, **98**, 9075–9087.
26. Sunshine, J. M. and Pieters, C. M., Determining the composition of olivine from reflectance spectroscopy. *J. Geophys. Res*., 1998, **103**, 13675–13688.
27. Cloutis, E. A., Pyroxene reflectance spectra: minor absorption bands and effects of elemental substitutions. *J. Geophys. Res.*, 2002, **107**(E6), 5039.
28. Schade, U., Wasch, R. and Moroz, L., Near-infrared reflectance spectroscopy of Ca-rich clinopyroxenes and prospects for remote spectral characterization of planetary surfaces. *Icarus*, 2004, **168**, 80–92.
29. Jackson, R. D., Clarke, T. R. and Moran, M. S., Bidirectional calibration results for 11 Spectralon and 16 $BaSO_4$ reference reflectance panels. *Remote Sensing Environ*., 1992, **40**, 2310–2319.
30. Longhi, I., Mazzoli, C. and Sgavettis, M., Determination of metamorphic grade in siliceous muscovite-bearing rocks in Madagascar using reflectance spectroscopy. *Terra Nova*, 2000, **12**, 21–27.
31. Harloff, J. and Arnold, G., Near-infrared reflectance spectroscopy of bulk analog materials for planetary crust. *Planet. Space Sci*., 2001, **49**, 191–211.
32. Longhi, I., Sgavetti, M., Chiari, R. and Mazzoli, C., Spectral analysis and classification of metamorphic rocks from laboratory reflectance spectra in the 0.4–2.5 mm interval: A tool for hyperspectral data interpretation. *Int. J. Remote Sensing*, 2001, **22**, 3763–3782.
33. Pompilio, L., Reflectance spectroscopy (VNIR) of igneous rocks: Characterization of the Bjerkreim–Sokndal cumulates, Ph D thesis, Parma University, Parma, Italy, 2005, p. 247.
34. Runciman, W. A., Sengupta, D. and Marshall, M., The polarized spectra of iron in silicates: I. Enstatite. *Am. Mineral*., 1973, **58**, 444–450.
35. Burns, R. G., Parkin, K. M., Loefler, B. M., Leung, I. S. and Abu-Eid, R. M., Further characterization of spectral features attributable to titanium on the moon. In Proceedings of the 7th Lunar and Planetary Science Conference, Houston, Texas, 1976, vol. VII, pp. 2561–2578.
36. Goldman, D. S. and Rossman, G. R., Determination of quantitative cation distribution in orthopyroxenes from electronic absorption spectra. *Phys. Chem. Miner*., 1979, **4**, 43–59.
37. Huguenin, R. L., Photostimulated oxidation of magnetite: kinetics and alteration phase identification. *J. Geophys. Res*., 1973, **78**, 8481–8493.
38. Hazen, R. M., Bell, P. M. and Mao, H. K., Effects of compositional variation on absorption spectra of lunar pyroxenes. In Proceedings of 9th Lunar Planetary Science Conference, Houston, Texas, 1978, pp. 2919–2934.

39. Gupta, R. P., *Remote Sensing Geology*, Springer-Verlag, Berlin, 2005, 2nd edn, p. 290.
40. Clark, B. E. and Johnson, R. E., http:people.Virginia.edu/~rej/Papers-Scan/Clark-Johnson-EOS 1996.pdf
41. Noble, S. K. and Pieters, C. M., Space weathering on Mercury: Implications for remote sensing. *Sol. Syst. Res.*, 2003, **37**, 31–35.
42. McCord, T. B. and Adams, J. B., Progress in remote optical analysis of lunar surface composition. *Moon*, 1973, **7**, 453–474.
43. Johnson, R. E. and Baragiola, R. A., Lunar surface: sputtering and secondary ion mass spectrometry. *Geophys. Res. Lett.*, 1991, **18**, 2169–2172.
44. Fischer, E. M. and Pieters, C. M., Remote determination of exposure degree and iron concentration of lunar soil using VIS–NIR spectroscopic methods. *Icarus*, 1994, **111**, 375–488.
45. Pieters, C. M. *et al.*, Space weathering on airless bodies: revolving a mystery with lunar samples. *Meteoritics Planet. Sci.*, 2000, **35**, 1101–1107.
46. Noble, S. K. *et al.*, The optical properties of the finest fraction of lunar soil: implications for space weathering. *Meteoritics Planet. Sci.*, 2001, **36**, 31–42.
47. Hapke, B., Space weathering from Mercury to the asteroid belt. *J. Geophys. Res.*, 2001, **106**, 10039–10073.
48. Allen, C. C., Morris, R. V., Lauer, H. V. and Mckay, D. S., Microscopic iron metal on glass and minerals – a toll for studying regolith maturity. *Icarus*, 1993, **104**, 291–300.
49. Allen, C. C., Morris, R. V. and Mckay, D. S., Experimental space weathering of lunar soils. *Meteoritics*, 1995, **30**, 479–480.

ACKNOWLEDGEMENTS. This work has been carried out with the support of ISRO PLANEX programme, coordinated by Physical Research Laboratory, Ahmedabad. The first author thanks the Council of Scientific and Industrial Research, New Delhi for providing Senior Research Fellowship.

Received 3 August 2009; revised accepted 8 December 2010

Erratum

Status of *Embelia ribes* Burm f. (Vidanga), an important medicinal species of commerce from northern Western Ghats of India

M. Mhaskar, S. Joshi, B. Chavan, A. Joglekar, N. Barve and A. Patwardhan

[*Curr. Sci.*, 2011, **100**, 547–552]

The photographs of *E. ribes* and *E. basaal* in Table 3 were interchanged. The following table presents corrected version.

Table 3. Comparative account of *Embelia ribes* with its allied species

Parameter	*Embelia ribes*	*Embelia basaal* (Syn. *Embelia tsjerium-cottam*, *Embelia robusta*)	*Maesa indica*	*Myrsine africana*
Habitat	Liana	Scandent shrub	Shrub	Shrub
Fruits	Black	Red	Green	Reddish-brown
Local name	Vavding	Vavding	Vavding	Vidanga/Chhota mendhru
Trade name	Kala Vavding	Lal Vavding	Vavding	Vidanga/Baibidanga
Unit price	Rs 110–160/kg, sometimes as high as Rs 326/kg (http://www.indiamart.com/chandraayurved/)	Rs 60–110/kg	Rs 25–30/kg	–
Embelin content (%)	2.3–3.1 (ref. 7)	1.6 (ref. 7)	Absent (ref. 29)	1.2–3.4 (ref. 10)
Extent of occurrence (km^2)	> 20,000	> 20,000	> 20,000	–
Occupancy (km^2)	10–500	> 2000	> 2000	–
Species population density	1–5/100 ha	2–5/ha	Not evaluated	–
Population decline/decade (%)	> 50	> 30	Not evaluated	–
Threat status (IUCN) according to CAMP	DD	VU	–	–
Threat	Habitat loss, local use, trade, immature harvest time	Habitat loss, destructive harvesting	–	–
Cultivation practice	Unknown	Unknown	–	–
Remarks	Rare, adulterants used, cultivation needs to meet current demand	Systematic cultivation practice needs to be standardized	Used as adulterant to *E. ribes*	Used as adulterant to *E. ribes* (ref. 30)
Image